

## GdN thin films: Bulk and local electronic and magnetic properties

F. Leuenberger,<sup>1</sup> A. Parge,<sup>1,2</sup> W. Felsch,<sup>1</sup> K. Fauth,<sup>3,4</sup> and M. Hessler<sup>3</sup>

<sup>1</sup>*I. Physikalisches Institut, Universität Göttingen, Friedrich-Hund-Platz 1, D-37077 Göttingen, Germany*

<sup>2</sup>*IV. Physikalisches Institut, Universität Göttingen, Friedrich-Hund-Platz 1, D-37077 Göttingen, Germany*

<sup>3</sup>*Physikalisches Institut, Universität Würzburg, Am Hubland, D-9704 Würzburg, Germany*

<sup>4</sup>*Max Planck Institut für Metallforschung, Heisenbergstrasse 3, D-70569 Stuttgart, Germany*

(Received 30 November 2004; revised manuscript received 7 April 2005; published 13 July 2005)

A study of high-quality thin films of the ferromagnet gadolinium nitride, GdN, is reported. The films, prepared by reactive ion-beam sputtering, show good stoichiometry and the lattice parameter, Curie temperature  $T_C$ , and saturation magnetization of the bulk material. The electrical conductivity is thermally activated down to the onset of magnetic ordering where there is evidence of a transition to metallic behavior. The transition can be tuned by a magnetic field, as reflected by a giant negative magnetoresistance. The ordered  $4f$  moment extracted from the spectra of x-ray magnetic circular dichroism at the gadolinium  $M_{4,5}$  edges is consistent with the  $^8S_{7/2}$  configuration of  $Gd^{3+}$ ; it varies with temperature as the macroscopic magnetization of the GdN layers. The experimental K-edge photoabsorption spectra of nitrogen in this compound indicate the presence of N  $p$  character of the low-lying unoccupied conduction-band states, pointing to hybridization of the N  $2p$  and Gd ( $5d, 6s$ ) states. However, a comparison of the spectra with the theoretical partial density of vacant N  $p$  states shows considerable disparities that are not well understood. The exchange field generated by the Gd  $f$  electrons in the ferromagnetic phase of GdN induces a magnetic polarization of the N  $p$  band states, as can be concluded from the observation of strong magnetic circular dichroism at the K edge of nitrogen. It indicates the presence of an important spin-orbit interaction in the final N  $p$  states.

DOI: [10.1103/PhysRevB.72.014427](https://doi.org/10.1103/PhysRevB.72.014427)

PACS number(s): 75.50.Pp, 78.70.Dm, 87.64.Ni, 71.30.+h

### I. INTRODUCTION

After a controversial discussion over the years<sup>1</sup> it seems to be recognized by now that stoichiometric GdN is a ferromagnet. It crystallizes in the simple face-centered cubic (fcc) structure of sodium chloride and the Curie temperature  $T_C$  is near 60 K.<sup>2</sup> These properties make it a close relative to the much-investigated isostructural EuO, which has similar fundamental electronic characteristics. EuO is one of the first ferromagnetic semiconductors discovered,<sup>3,4</sup> with a band gap of about 1.2 eV and a Curie temperature comparable to that of GdN. Both compounds have a strongly correlated electron structure, with an identical  $^8S_{7/2}$   $4f$  shell configuration entailing zero orbital angular momentum. However, dissimilarities in the electronic correlations in the solids ascribed to different relative energy positions of the  $4f$  levels<sup>5</sup> lead to substantial disparities in the magnetic and transport properties of the two compounds. There is a large uncertainty about the electronic ground-state configuration of GdN. Band structure calculations [density functional theory with a local spin density approximation (LSDA) for the exchange correlation energy, treating the Gd  $4f$  states as core states]<sup>6</sup> predict a transition from a *semiconductor* in the paramagnetic phase, with an indirect narrow energy gap between the bottom of the conduction bands at the  $X$  point of the Brillouin zone (predominantly  $5d_{2g}$  derived) and the top of the valence bands at the  $\Gamma$  point (essentially N  $2p$  derived), to a *semimetal* in the ferromagnetic phase, with a low concentration of free charge carriers (a few percent per Gd ion). The gap is expected to be sensitive to magnetic ordering or external magnetic fields. It has been speculated<sup>7,6</sup> that semimetallic overlap might occur for one spin channel only. GdN then would be a *half metal*

with complete spin polarization. This becomes strong support for recent more advanced *ab initio* calculations by Aerts *et al.*<sup>8</sup> of the GdN ground-state electronic structure, using the self-interaction corrected (SIC) LSDA. These calculations, being part of a systematic study of the entire rare-earth nitride series, predict an (indirect) band gap of  $\sim 0.9$  eV for the minority spin channel only, and a principal Gd ( $s, d$ ) and N  $p$ -like symmetry of the majority electrons at the Fermi energy  $E_F$ . If the suspected half-metallic character is verified, the compound will be of considerable interest for potential application in spin-filtering devices, since it will combine the ability to spin polarize electrons with an expected good spin injection efficiency into semiconductors. A barrier for such applications might be the low Curie temperature and the predicted<sup>8</sup> low density of the fully spin-polarized states at  $E_F$ . Ordered magnetism of GdN is dominated by the large local spin magnetic moments of the half-filled Gd  $4f$  shell coupled by indirect exchange interactions. There are small magnetic contributions, resulting from hybridization and exchange, from the Gd ( $s, d$ ) and N  $p$  band electrons. This indicates that the N  $p$  states lie in the same energy range as the valence Gd states. The itinerant magnetic moments induced on the Gd  $5d$ -derived and N  $2p$ -derived states are expected to oppose each other and to nearly cancel.<sup>6,8,9</sup> Hence the net spontaneous magnetic moment of GdN results from the Gd  $4f$  shell only. As the conductivity properties are determined by the electrons in the ( $5d, 6s$ ) conduction bands, which are hybridized with the N  $2p$  band, the magnetism induced on the band states through the  $4f$  states, although small, is expected to lead to observable effects in magnetotransport. Most of the theoretical predictions remain to be verified experimentally. To our knowledge, nothing has been

reported in the literature to determine the electronic structure of GdN using modern methods such as electron spectroscopy.

The lack of sufficient reliable experimental information on the fundamental properties of GdN is related to the problem of sample preparation.<sup>2</sup> The high melting point makes it very difficult to grow crystals with good stoichiometry and well-defined properties. The early discrepancies concerning the magnetic ground-state configuration (ferromagnetic<sup>10-13</sup> or antiferromagnetic<sup>1,14</sup>), for example, may be related to a different degree of sample perfection. The experimental situation is at variance with the other Gd mononitrides. High-quality single crystals have been grown of these compounds and well-characterized experimentally.<sup>2,15-17</sup> It is generally accepted that they are antiferromagnetic semimetals.<sup>2,15,16</sup> Understanding the different magnetic order in GdN is a challenge. The compound has attracted particular attention, last but not least in view of the similarities and differences with respect to the related compound EuO. In a phenomenological explanation of the different magnetic ground state configurations in the Gd mononitrides one assumes that the exchange interaction coupling the  $4f$  magnetic moments in these compounds consists of two competing terms,<sup>2</sup> as proposed in early models also conceived for the Eu monochalcogenides:<sup>18-21</sup> a ferromagnetic and an antiferromagnetic one,  $J_1$  and  $J_2$ , related to the nearest and next-nearest rare-earth-ion neighbors, respectively. In these models,  $J_1$  represents indirect exchange essentially mediated by  $5d$  orbitals of the cations ( $f$ - $d$  exchange),  $J_2$  represents superexchange via the  $2p$  orbitals of the anions. The different sensitivities of the two exchange parameters to the interatomic distances are the crucial point that is invoked to explain the change of magnetic order when going from GdN to the other members of the Gd pnictides: only in GdN the ferromagnetic exchange,  $J_1$ , dominates the magnetic ground state configuration.<sup>2</sup> Explaining  $J_1$  on a microscopic basis is a difficult task, in particular for GdN. A microscopic model was developed by Kasuya.<sup>5</sup> He compares the indirect interactions in GdN and EuO and concludes that there are substantial disparities, which are related to differences of the band states near the Fermi energy.

This paper reports on the magnetic and transport properties of high-quality thin films of GdN prepared by  $N^+$  plasma-assisted reactive sputtering. The samples provide a very good medium for studying the intrinsic properties of the compound. They show good stoichiometry, the Curie temperature  $T_C$  of the bulk material, and the Hund's rule value of the magnetic saturation moment ( $\sim 7 \mu_B/\text{Gd ion}$ ). The electrical conduction is thermally activated down to  $T_C$ , which is evidence of a transition to metallic behavior. The transition is considerably shifted in a sufficiently high magnetic field, as it is reflected in a giant magnetoresistance. Core-level x-ray absorption (XA) spectroscopy near the nitrogen  $K(1s \rightarrow 2p)$  edge together with a measurement of circular magnetic dichroism (XMCD) was used to study the  $N p$  character of the low-lying unoccupied electronic conduction band states of GdN, which is present because of the covalent mixing between the  $N 2p$  and Gd ( $5d, 6s$ ) states, as well as the expected magnetic polarization of the  $N p$  states in the ferromagnetic phase.<sup>8</sup> The XMCD technique was also

applied to the gadolinium  $M_{4,5}(3d \rightarrow 4f)$  photoabsorption edges to study the magnetic polarization of the Gd  $4f$  moments. As expected, it mirrors the behavior of the macroscopic magnetization of the GdN layers.

The remainder of the paper is organized as follows. After a brief description of the preparation of the GdN layers, of the experimental methods used, and of some basic sample characteristics in Sec. II, in Sec. III we present and discuss the experimental results obtained on the electronic and magnetic properties by bulk magnetometry, electrical resistance measurements, and x-ray spectroscopy. We conclude the paper in Sec. IV.

## II. EXPERIMENTAL

The GdN film samples with thickness up to 2000 Å were grown by reactive ion-beam sputtering of Gd in an ultra-high vacuum chamber (base pressure  $< 5 \times 10^{-10}$  mbar). A Kaufman-type ion source was used with argon as a sputtering gas. The growing film was exposed to a nitrogen beam with thermal energy provided by an ECR plasma source dissociating the  $N_2$  molecules into radicals to improve the reaction with Gd. During growth the background partial pressure of nitrogen was near  $2 \times 10^{-5}$  mbar, as that of Ar, and that of reactive gases ( $O_2$ , CO) was below  $10^{-10}$  mbar. Si(100) wafers served as substrates. They were coated with a 40 Å thick Cr or W buffer to avoid reaction with GdN and kept at 450 °C during film growth. Typical growth rates were near  $0.5 \text{ Å s}^{-1}$ . The samples were terminated with a Cr or Al cap layer (up to 50 Å thick) deposited at room temperature to prevent oxidation upon exposure to air, inevitable for the experiments *ex situ*. High-purity gases Ar (6N) and  $N_2$  (6N) and target metals Gd (3N), Cr (4N), W (4N), and Al (4N) were used.

The cleanliness and stoichiometry of the GdN layers was checked by x-ray photoelectron spectroscopy (XPS) *in situ* after preparation, using an Al  $K\alpha$  x-ray source and a hemispherical electron energy analyzer. This technique was also used to probe the electronic structure in the valence band region. The resolution of the measurement was about 1 eV. The XPS spectra revealed that the layers are free of oxygen impurities (the oxygen concentration is below 0.05%, the sensitivity of the spectrometer). Moreover, analysis of the Gd  $4d$  and N  $1s$  emission intensities confirms good stoichiometry. This is verified further by an analysis based on the resonant nuclear reaction  $^{15}\text{N}(p, \gamma\alpha)^{12}\text{C}$ . The two methods permit us to conclude then that deviations from the stoichiometric one-to-one composition ratio of the GdN layers are at most a few percent.

Structural characterization was performed by x-ray diffraction. Bragg scans recorded along the normal of the GdN layers reveal polycrystalline growth in the NaCl structure with a lattice parameter  $\sim 1.5\%$  above that of the bulk material,<sup>2</sup> without foreign phases. The average extension of the grains in the growth direction, calculated from the full width at half maximum of the diffraction peaks using Scherrer's formula, amounts to  $\sim 100 \text{ Å}$ .

Standard techniques of vibration sample magnetometry (VSM), superconducting quantum interference device

(SQUID) magnetometry, and the magneto-optical Kerr effect (MOKE) in a longitudinal setup were used to measure the macroscopic magnetization of the layers.

The XA and XMCD spectra were acquired at the soft x-ray beamline PM3 of the BESSY storage ring in Berlin at temperatures between 15 K and 300 K. The beamline supplies a monochromatic beam by a grating monochromator with a resolution of  $\sim 0.1$  eV in the energy range of interest ( $\sim 350$  to  $1250$  eV); it results from a bending magnet and is 95% circularly polarized. Electronic transitions from the Gd  $3d$  and N  $1s$  states into dipole allowed unoccupied states with  $f$  and  $p$  character, respectively, were studied. The spectra were obtained in an UHV system (base pressure  $< 10^{-10}$  mbar) by measuring the total electron yield (TEY) and are estimated to sample the top  $\sim 50$  Å of the layers. The UHV environment warrants a clean sample surface during data acquisition. Unfortunately, the protective Cr cap layer attenuates the TEY signal from the buried GdN layer considerably. This is a crucial point for the XMCD spectra taken at the N K edge since the dichroic signal is very small. Therefore, the thickness of the Cr layer (originally 30 Å) was reduced to about one half by moderate  $\text{Ar}^+$  ion etching at grazing incidence *in situ* in the UHV preparation chamber of the beamline. The thickness reduction was monitored by the decrease of the XA signal at the Cr  $L_3$  edge. The cap was not removed completely to avoid damaging of the GdN layer surface by introducing defects or stoichiometry changes.

XMCD experiments probe the absorption cross section at a core level threshold of a material with a net magnetic moment for two opposite relative orientations of the magnetization and helicity of circularly polarized photons. The difference of the spectra measures the net magnetic moment through transfer of the x-ray angular momentum vector in the absorption process. Due to the creation of a core hole this technique is site and orbital selective. Sum rules<sup>22</sup> relate the integrated dichroic signals for a given spin-orbit split absorption edge to local spin and orbital contributions to the ground-state magnetic moment. In our study, the XMCD spectra of the GdN layers were recorded in the TEY mode at constant beam helicity by scanning the photon energy across a given absorption edge for two opposite directions of the saturation magnetization induced by applying an external magnetic field (10 kOe) parallel and opposite to the x-ray propagation direction; it was oriented at an angle of  $30^\circ$  with respect to the layer surface and inverted at each energy point. The XMCD signal is the difference between the normalized absorption signals for the two field directions,  $I^+$  and  $I^-$ .

The XMCD technique can be used to measure element-resolved hysteresis curves of the GdN layers:<sup>23</sup> a loop recorded at the peak energy of the dichroic signals at the Gd  $M_4$  and N K edges, respectively, by varying the external field between 0 and  $\pm 1$  T was corrected for the (magnetic-field-dependent) nonmagnetic contribution to the TEY signal by a loop measured just below the edge where magnetic dichroism is absent.

Indirect XA measurements performed in the TEY mode generally suffer from saturation and self-absorption effects expected to be present when the photon penetration depth becomes comparable to the electron or photon escape depths.<sup>24</sup> Depending on the geometry of the experiment,

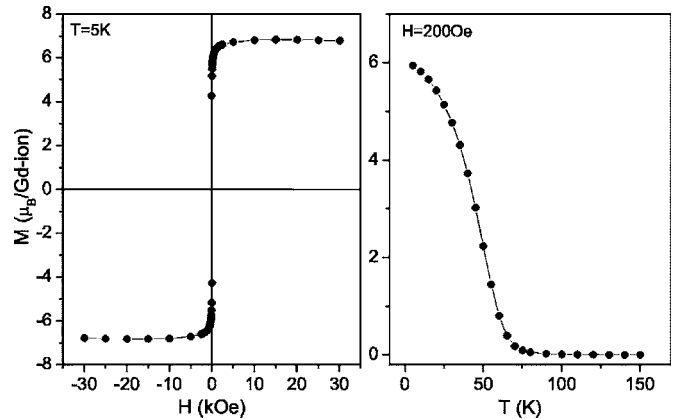


FIG. 1. Magnetization of a sample  $\text{Si}(100)/\text{Cr}(50 \text{ \AA})/\text{GdN}(500 \text{ \AA})/\text{Al}(30 \text{ \AA})$  as a function of magnetic field at 5 K (left panel) and as a function of temperature in a magnetic field of 200 Oe (right panel); data corrected for contributions of substrate, buffer, and capping layer. The error in the magnetization data is  $\sim 5\%$ .

these effects can distort the spectra and/or reduce their intensity. Corrections for such effects are particularly crucial if quantitative values of the magnetic moments, especially of the orbital moments, are to be extracted from the XMCD spectra by using the magneto-optical sum rules. Here, such corrections were easily made for the Gd- $M_{4,5}$  TEY absorption spectra by a direct comparison with spectra measured in transmission mode.<sup>25</sup> For the N K edge, such direct transmission XA spectra are not available. In this case corrections for self-absorption were not made.

### III. RESULTS AND DISCUSSION

#### A. Bulk magnetic and transport properties

Conventional magnetometry identifies the GdN layers as good ferromagnets, with a spontaneous magnetization and a Curie temperature in close agreement with the values of the bulk stoichiometric compound obtained by the Sendai group.<sup>2</sup> This is an important point in view of the early controversial results documented in the literature about the magnetic ground state of this material<sup>1,10-14</sup> and a proof of the good quality of the samples. Figure 1 shows the magnetization of a 500 Å thick GdN layer vs magnetic field applied in the plane at 5 K (left panel) and the magnetization at a field of 200 Oe vs temperature (right panel). The spontaneous magnetization extracted from the low-temperature magnetization curve is  $(6.8 \pm 0.3) \mu_B/\text{Gd ion}$  in agreement with the theoretically expected  $7.0 \mu_B/\text{Gd}^{3+}$  for a half-filled  $4f$  shell. The experimental error essentially results from the estimation of the volume of the layer. Note that Li *et al.*<sup>2</sup> report a saturation moment of  $6.84 \mu_B/\text{Gd ion}$  for bulk GdN. The result indicates that there is no net contribution to the spontaneous magnetization from the conduction bands in this compound, in agreement with theoretical prediction.<sup>6,9</sup> It is in contrast to magnetism of Gd metal, where an induced spin polarization of the ( $5d, 6s$ ) conduction bands contributes  $\sim 0.6 \mu_B/\text{ion}$  to the saturation moment at low temperature,

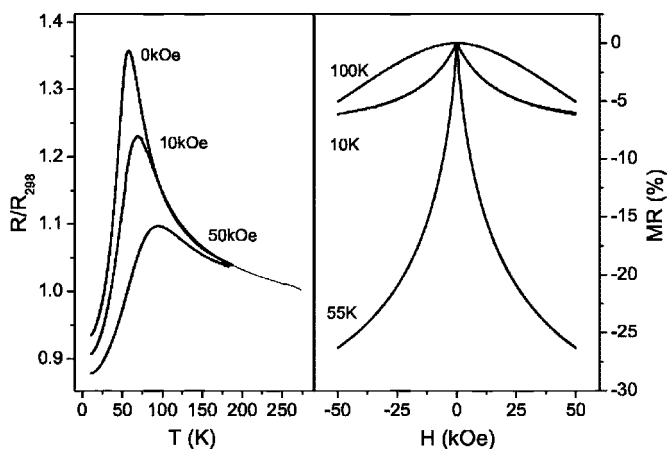


FIG. 2. Resistance (normalized with the value at 298 K) of a 1000 Å thick GdN film as a function of temperature in different magnetic fields (left panel). The resistivity at 298 K is  $\sim 10$  mΩ cm. Right panel: Magnetoresistance  $(R(H)-R(0))/R(0)$  vs magnetic field at temperatures below, near, and above the Curie temperature  $T_C$ .

amounting to  $\sim 7.6 \mu_B/\text{ion}$  then.<sup>26</sup> The magnetization curve  $M(H)$  in Fig. 1 (left panel) indicates that the GdN layer is magnetically soft; the coercivity amounts to 75 Oe. Magnetic saturation is reached near an external field of 5 kOe; for  $H=200$  Oe, the magnetization at 10 K amounts to  $\sim 6 \mu_B/\text{Gd ion}$  already (right panel). This confirms the absence of oxygen impurities as also recognized in the XPS spectra. In fact, it has been found previously that GdN is difficult to magnetize to saturation when doped with such impurities: the saturation field of a sample  $\text{GdN}_{0.96}\text{O}_{0.04}$  at 4.2 K exceeds 50 kOe, and at 200 Oe a magnetization inferior to  $0.2 \mu_B/\text{Gd ion}$  is reached.<sup>1</sup>

It can be concluded from the temperature dependence of the low-field magnetization in Fig. 1 that the Curie temperature  $T_C$  of the GdN layer must be close to 60 K. A more precise value results from an Arrott plot:<sup>27</sup> it yields  $T_C = (58.6 \pm 1)$  K for the 500 Å thick GdN layer of Fig. 1, which is in excellent agreement with the value 58 K obtained by Li *et al.*<sup>2</sup> for a bulk stoichiometric sample of GdN.  $T_C$  depends only weakly on the thickness of the GdN layers. The Curie temperatures of 50 and 20 Å thick samples, for example, are only 1.5 and 3.5 K below the “bulk” value obtained for the 500 Å thick layer, respectively. Hence the phase transition to ferromagnetism is fairly insensitive to reduced dimensionality for this compound. This is at variance with the more pronounced thickness dependence of  $T_C$  which is theoretically expected for films of ions with  $S=7/2$  local moments on a fcc lattice, modeled by Heisenberg exchange interactions.<sup>28</sup> Experimental verifications for EuO films, which the authors had in mind, are unknown to us. Considering our data, it appears that the underlying model of the magnetic interactions may not be applicable to GdN.

An important quantity closely related to the electronic structure of GdN is the variation of the electrical resistivity with temperature and external magnetic field. Figure 2 (left panel) shows the electrical resistance of a GdN layer as a function of temperature in zero magnetic field, and in  $H$

$= 10$  and 50 kOe. In zero field, there is a pronounced resistance peak at the Curie temperature of the compound indicating a strong influence of the magnetic phase transition on electrical transport. The resistance is affected appreciably by the external magnetic field; it reduces the peak at  $T_C$  and shifts the magnetic transition to higher temperatures. The result is a very large negative magnetoresistance near  $T_C$  (Fig. 2, right panel). Above  $T_C$ , the conductivity is thermally activated, with carrier activation energy near 10 meV in zero field. This suggests highly degenerate  $n$ -type semiconducting behavior, presumably due to small deviations from stoichiometry, i.e., nitrogen vacancies acting as shallow donors. Below  $T_C$ , the conduction becomes nonactivated, suggesting a transition to a metallic ground state predicted by Aerts *et al.*<sup>8</sup> A semiconductor-metal transition driven by a phase transition to ferromagnetic order is an outstanding property of europium-rich EuO.<sup>29,30</sup> Together with a large magnetoresistance, it is largely responsible for the early widespread interest in this compound. The effect is not intrinsic in origin, but is related to nonstoichiometry of EuO and involves extra electrons, which are believed to be provided by oxygen vacancies acting as shallow donors.<sup>29,31</sup> An early explanation<sup>31</sup> of the semiconductor-metal transition in EuO may equally apply to GdN: Above  $T_C$ , the donor impurity levels are located in the energy gap slightly below the low-lying  $\text{RE-}5d_{t_2g}$  dominated conduction band states. Electrons may be promoted into the conduction band from the defect states by thermal activation, producing semiconducting behavior. In the ferromagnetic phase below  $T_C$ , the conduction band experiences exchange splitting. The donor impurity levels now are crossed by the conduction band edge (eventually by the majority spin-state subband only) and release electrons to this band where they can propagate and produce metallic conductivity. A different model invoked for a qualitative explanation of the resistivity anomalies in nonstoichiometric Gd monopnictides (exempting GdN) is magnetic polaron formation.<sup>16</sup> If it plays a role in the GdN layers discussed here is an open question.

It must be pointed out that in nonstoichiometric EuO the resistance drop upon the transition to the ferromagnetic state is much more pronounced than in the GdN layers. Also, the activation energy in the paramagnetic regime is much higher, being typically  $\sim 0.3$  eV.<sup>32</sup> However, the overall conductivity behavior of the GdN layers basically is rather similar. The differences may be related to different degrees of nonstoichiometry, the different nature of the vacancies, a different importance of impurity scattering for the conduction below  $T_C$ , and/or the differences in the fundamental electronic structure of the compounds. We may conclude that, as in EuO, ferromagnetic order in the GdN layers causes a semiconductor-metal transition.

## B. Local electronic and magnetic properties: X-ray absorption and x-ray magnetic circular dichroism spectroscopy

Magnetism of GdN is determined by the large spin magnetic moment of the highly localized  $4f$  electron states. The recent *ab initio* band structure calculations of Aerts *et al.*<sup>8</sup> result in (*i*) occupied majority-spin  $f$  states that form a nar-

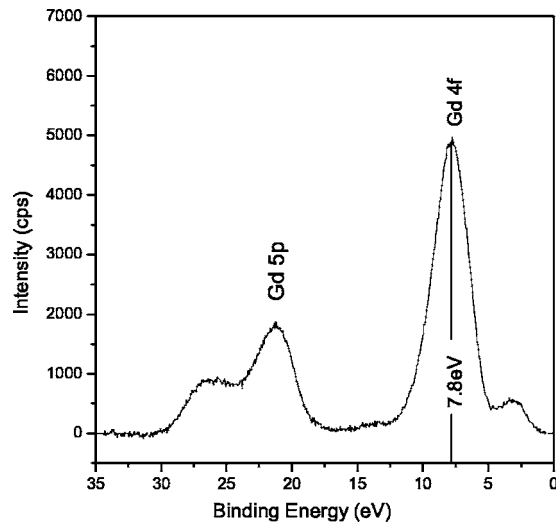


FIG. 3. XPS spectrum of GdN in the valence-band region showing the energy positions of the gadolinium  $5p$  and  $4f$  emissions. The intensity immediately below the Fermi level, with a broad maximum near 3 eV, predominantly represents the nitrogen  $p$  states. Measurement at room temperature on a 500 Å thick layer *in situ* after preparation.

row band well below the Fermi energy and have the characteristics of core states; (ii) minority-spin  $f$  states located somewhat above  $E_F$  with band-like character that allows hybridization with the unoccupied N  $p$  states. The majority  $f$  electrons create an exchange field that leads to spin splitting of the N  $p$  band. Furthermore, the majority-spin N  $p$  band hybridizes with the Gd ( $s, d$ ) bands. One of the consequences is that the N anion should carry a magnetic moment. We shall demonstrate in the following that light is shed on these predictions by the results of high-energy electron spectroscopy.

An important issue is the energy position of the occupied  $f$  states in the electron band structure of GdN. Figure 3 shows the XPS spectrum in the valence band region. The prominent peak located at  $\sim 8$  eV below the Fermi level represents the  $\text{Gd}^{3+} 4f^6$  final state multiplet.<sup>33</sup> This value, determined here for the first time for this compound, fits nicely into the window reported for the location of the  $4f$  emission in the XPS spectra of the other Gd monopnictide single crystals.<sup>17</sup> It is well known that the  $4f^6$  final state energy position cannot be simply identified with that of the occupied  $f$  states in the ground state bands of the materials because of relaxation (screening) effects. Concerning GdN, Aerts *et al.*<sup>8,34</sup> find 14.5 eV below the Fermi level as the  $f$  location in the calculated ground state density of occupied states, suggesting a relaxation energy of about 7 eV for this system. If this is a reasonable estimate is an open question.<sup>35</sup> It is interesting to point out that the energy location of the  $4f$  emission in the spectrum of GdN in Fig. 3 is distinctly different from the position of the occupied  $4f$  level in semiconducting EuO found in the band gap slightly above the upper valence band edge by photoemission measurements.<sup>36</sup> This has important consequences for the electronic interactions of the two compounds, as discussed by Kasuya.<sup>5</sup>

Since ordered magnetism in GdN, macroscopically reflected in Fig. 1, is  $4f$  electron dominated it is essential to

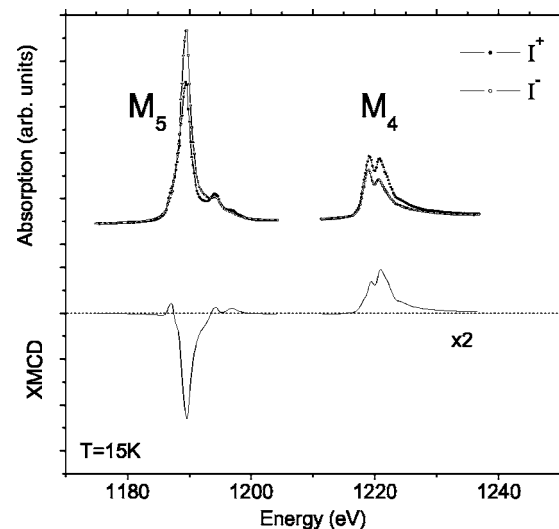


FIG. 4. X-ray absorption spectra,  $I^+$  and  $I^-$ , at the gadolinium  $M_{4,5}$  edges of a GdN layer (1000 Å) measured in TEY mode at 15 K in an external field of  $\pm 10$  kOe parallel (intensity  $I^+$ ) and antiparallel (intensity  $I^-$ ) to the propagation direction of the light with fixed circular polarization (top) and related XMCD spectrum, ( $I^+ - I^-$ , intensity multiplied by 2).

locally probe the character of the Gd  $4f$  states. This can be achieved by XA spectroscopy and XMCD at the  $M_{4,5}$  absorption edges of Gd which access the  $4f$  states by the dipole-allowed  $3d \rightarrow 4f$  resonant transition. Representative spectra recorded in TEY mode on a GdN film held at 15 K are displayed in Fig. 4. General shape and structure (position in energy, relative intensities) and magnetic field dependence are characteristic of  $\text{Gd}^{3+}$  ions, as expected.<sup>37</sup> There are no similarities with the corresponding spectra of EuO films, which recently were found to show very anomalous features that remain to be explained.<sup>38</sup> The dichroism effect is large, as is common for Gd-based systems at the  $3d$  threshold; it amounts to more than 20%. Applying the sum rules<sup>22</sup> to the XMCD spectra (properly normalized to the isotropic signal and corrected for incomplete photon polarization) we find that the ordered  $4f$  spin moment is close to  $7 \mu_B/\text{Gd}$  ion and the  $4f$  orbital moment is near zero with good accuracy, which is consistent with the  $^8S_{7/2} (4f^7)$  configuration of the Gd ion. Moreover, the integrated XMCD signals measured at different temperatures closely follow the thermal variation of the macroscopic magnetization of GdN (in the same magnetic field of 10 kOe, not shown).

Existing band structure calculations emphasize that the electronic states of nitrogen are fundamentally involved in the formation of magnetic order in GdN.<sup>6-9</sup> In fact, the exchange field established by the  $f$  electrons in the ferromagnetic state is expected to induce a magnetic polarization of the N  $p$  band, which is reflected in a spin splitting of the DOS<sup>8</sup> (see Fig. 7 below). It is interesting to compare this theoretical result with the measured XA spectra and XMCD at the N K edge. These spectra are dominated by the dipole-allowed  $1s \rightarrow 2p$  resonant transition and hence directly probe the  $2p$  character of the unoccupied low-lying conduction band states at the N site and their magnetic polarization. Figure 5 displays the XA spectrum and the related XMCD

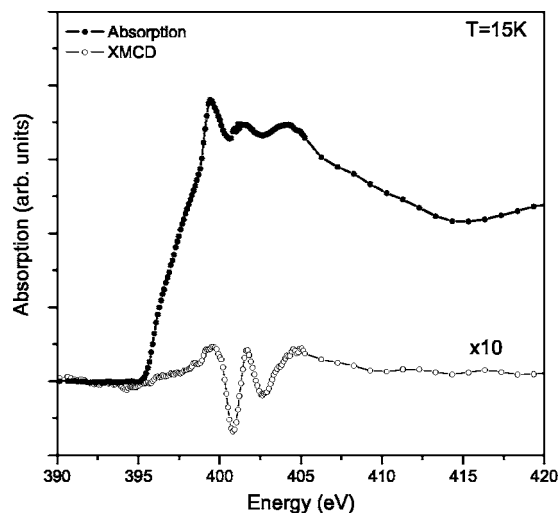


FIG. 5. Isotropic x-ray absorption spectrum,  $(I^+ + I^-)/2$ , at the nitrogen K edge of a GdN layer (500 Å) measured in TEY mode at 15 K, recorded in an external field of  $\pm 10$  kOe applied at  $30^\circ$  with respect to the layer normal, parallel (intensity  $I^+$ ) and antiparallel (intensity  $I^-$ ) to the propagation direction of the light with fixed circular polarization (top) and related XMCD spectrum ( $I^+ - I^-$ , intensity multiplied by 10).

spectrum of a GdN layer measured at 15 K in TEY mode. The XA spectrum exhibits three distinct maxima just above the absorption edge separated by a few eV. It is worth noting that it varies little when the temperature is raised to 300 K. The dichroic spectrum is clearly resolved. Its peak amplitude amounts to  $\sim 4\%$  of the edge jump of the isotropic XA spectrum at 415 eV, which is a remarkably large value for K-edge XMCD. It is documented that sizeable XMCD signals can be detected at the K edge of “nonmagnetic” atoms, like sulfur and oxygen in ferromagnetic EuS (Ref. 39) and EuO,<sup>40</sup> respectively. The N K-edge dichroic signal in GdN is about three times larger than at the K edge of oxygen in EuO and exceeds that at the K edge of sulphur in EuS by an order of magnitude; it surpasses even that at the K edge of iron metal.<sup>41</sup> As can be seen in Fig. 5, the magnetic dichroism sets in together with the onset of the absorption and slowly rises with photon energy up to  $\sim 400$  eV. This is followed by pronounced spectral features that appear as two derivative-like structures related to the second and third peaks in the spin-averaged XA spectrum. The XMCD signal is not ambiguous, as was reflected by its near-perfect inversion when the helicity of the light was reversed. Its intensity decreases with increasing temperature and disappears above  $T_C$ . We further point out that the validity of the XMCD spectrum is confirmed by measurements of electronic-shell selective hysteresis loops. This can be concluded from the comparison of such loops measured by XMCD at the  $M_4$  edge of Gd and the K edge of N on the same GdN layer sample (Fig. 6). Due to the relatively small dichroic signal at the N K edge compared to that at the Gd  $M_4$  edge, the magnetic hysteresis loop of the N  $2p$  magnetic moment is more noisy, but it follows nicely the magnetic field dependence of the Gd  $4f$  moment, which is an almost perfect image of the hysteresis loop of macroscopic sample magnetization (Fig. 1). This means that

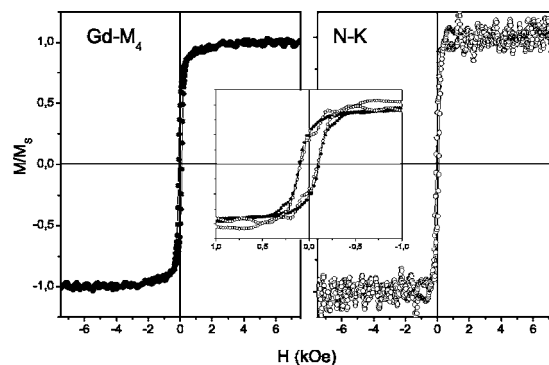


FIG. 6. Element- and symmetry-resolved hysteresis loops measured on a GdN layer (500 Å) at 15 K. Shown is the magnetic-field dependence of the TEY XMCD signals at the maximum of the Gd- $M_4$  edge (left) and the lowest minimum of the N-K edge (right). Middle: expanded representation of the loops in a smaller magnetic-field range.

the Gd  $4f$  magnetization as well as the induced N  $2p$  magnetization, measured locally by the XMCD technique, not only are closely interrelated but represent the bulk magnetization of the entire GdN layer.

Quite generally, the occurrence of magnetic dichroism in x-ray absorption originates from the spin polarization of the empty electron states addressed and the presence of spin-orbit (SO) interaction. At the K edges, SO coupling is only relevant in the final  $p$ -projected state since this interaction is absent in the initial  $s$  state. It is well known from theoretical considerations<sup>42–44</sup> that in this case the XMCD signal measures the magnetic orbital polarization of the unoccupied  $p$ -symmetry states on the core-hole site. Hence in the present case the observed N K-edge XMCD is to be ascribed to an important SO interaction in the N  $2p$  final state in ferromagnetic GdN. Since N is a light element it can be ruled out that the  $2p$  orbital moment is generated by the spin polarization of the  $2p$  states through SO interaction within the anion. Rather, it must be assumed that it is induced by the orbital polarization of the  $5d$  states on adjacent Gd sites via  $2p$ - $5d$  hybridization. Such  $p$ - $d$  mixing mechanism and orbital moment transfer have been recently discussed, for example, for the K-edge XMCD of O in EuO (Ref. 40) and of Ga in ferromagnetic  $Mn_3GaC$ .<sup>45</sup> Its importance was similarly emphasized some time ago for the K-edge magnetic dichroism of Fe and Ni.<sup>42</sup> It is worth noting that preliminary measurements of XMCD at the  $L_{2,3}$  absorption edges of Gd in GdN layers indicate a magnetic polarization of the Gd  $5d$  states.<sup>46</sup> It is well known that in Gd-based systems these states interact strongly with the  $4f$  states, hence application of the sum rules<sup>22</sup> is excluded.<sup>47</sup> This means that information on the orbital polarization of the  $5d$  states that would be useful to elucidate the mechanism for the N  $2p$  orbital polarization cannot be obtained from these spectra.

The XA spectrum in Fig. 5 evidences significant N  $2p$  hole character of the low-lying unoccupied conduction band states of GdN, induced by N  $2p$ -Gd  $5d$  hybridization. A comparison with the SIC-LSDA ground state electronic structure calculations of Aerts *et al.*<sup>8,34</sup> is an important issue. Figure 7 displays the calculated (spin-resolved) N  $p$ -projected density

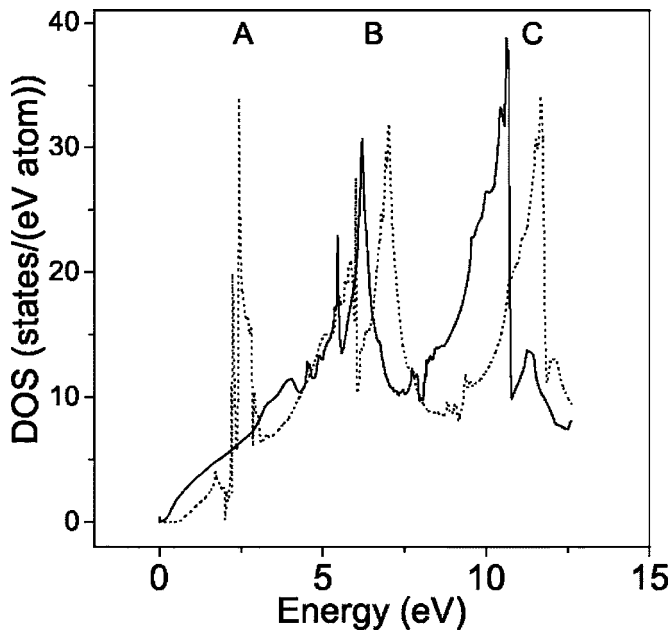


FIG. 7. Nitrogen  $p$ -projected density of electron states in the ground state of GdN above the Fermi energy  $E_F$  (denoted as the zero of energy) calculated by Aerts *et al.* (Ref. 34). Full lines represent majority spin, dashed lines minority spin.

of unoccupied states (DOS) of GdN above the Fermi energy  $E_F$ . These states lie in the same energy range as the vacant Gd  $5d$ -projected states.<sup>34</sup> The N  $p$  DOS shows a distinct narrow peak (labeled A) around 2.5 eV above  $E_F$  in the minority spin channel which is attributed to a strong hybridization of unoccupied Gd  $f$  minority spin states with N  $p$  states in this correlated system.<sup>8</sup> There are two additional peaks (B and C) in both spin channels at energies somewhat above 5 and 10 eV, respectively. Inspection of the N K-edge XA spectrum in Fig. 5 reveals that in spite of the three-peak structure of its line shape, the correspondence with the calculated N  $p$  DOS is not obvious since the energetic distances of the peaks do not match, nor do the absolute positions. [We locate the zero of energy ( $E_F$ ) of the DOS curve at the onset of absorption.] There is no evidence in the measured spectrum of the  $f$ -related DOS signature A near 2.5 eV. It is unlikely that this feature should be identified with the first maximum in the spectrum at  $\sim 400$  eV since it lies too high in photon energy. On the other hand, this maximum apparently has no correspondence in the calculated N  $p$  DOS.

We mention that the spectral feature at  $\sim 400$  eV (Fig. 5) was not contained in a preliminary N K-edge XA spectrum recorded on a Cr-covered (30 Å) GdN layer using the total fluorescence yield (TFY) detection mode. Due to the larger probing depth of this method compared to the TEY detection, this spectrum is a signature of the bulk GdN XA behavior of the sample. If reproducible, this result would indicate that the first maximum above the edge in the XA spectrum in

Fig. 5 might be related to the GdN surface or interface with the Cr capping layer where the TEY detection is sensitive. This would also apply for the slowly rising part of the XMCD signal below  $\sim 400$  eV. But the TFY result has to be verified before a definite conclusion can be drawn.

When comparing XA spectra with band structure calculations it should be noted that the interaction between the core hole and the electron excited into the conduction band in principle can lead to excitonic effects in the spectra. However, adopting an argument Steeneken *et al.*<sup>40,48</sup> applied to the oxygen K-edge XA spectra of the closely related compound EuO, since the conduction band essentially is Gd  $5d$  derived and the excited electron therefore will be effectively separated from the nitrogen atom, its interaction with the N  $1s$  core hole will be so small as compared to the conduction band width that its effect will be negligible.

#### IV. CONCLUSION

Experimental results concerning the structure, electrical conductivity, and magnetization show that ferromagnetic GdN films of good quality may be prepared. A number of theoretical predictions for this material were confirmed. X-ray absorption spectra recorded at the K edge of nitrogen clearly indicate the presence of low-lying unoccupied N  $p$ -derived states in the conduction band. Discrepancies between the spectral line shape and the recently calculated<sup>34</sup> N  $p$ -projected density of unoccupied states above the Fermi energy are unexplained, as is the relation between the positions of the occupied Gd  $4f$  states in the theoretical ground state energy bands and in the experimental valence band XPS spectrum. The observation of strong magnetic-circular dichroism at the N-K edge below the Curie temperature reveals that (i) the N  $p$  states are magnetically polarized and (ii) that these states experience a distinct spin-orbit interaction. To understand its origin further theoretical work is mandatory. Element-specific XMCD hysteresis loops mirror a close correlation between the local ordered N  $2p$  and Gd  $4f$  magnetism and the bulk magnetization. We believe that the present study will contribute to the basic understanding of GdN. It is clear that many questions remain unanswered, like the one concerning the predicted half metallicity of this compound.

#### ACKNOWLEDGMENTS

We are grateful to C. Aerts and P. Strange for kindly providing detailed unpublished theoretical results on the density of electron states (element, symmetry, and spin resolved) of GdN. Enlightening discussions with H. Ebert, G. Krill (Orsay), and K. Samwer are gratefully acknowledged. We thank the beamline staff at BESSY II for technical support. This work was supported by the Deutsche Forschungsgemeinschaft within SFB 602.

- <sup>1</sup>P. Wachter and E. Kaldis, *Solid State Commun.* **34**, 241 (1980)
- <sup>2</sup>D. X. Li, Y. Haga, H. Shida, T. Suzuki, Y. S. Kwon, and G. Kido, *J. Phys.: Condens. Matter* **9**, 10777 (1997).
- <sup>3</sup>B. T. Mathias, R. M. Bozorth, and J. H. van Vleck, *Phys. Rev. Lett.* **7**, 160 (1961).
- <sup>4</sup>P. Wachter, in *Handbook of Physics and Chemistry of Rare Earths*, edited by K. A. Gschneidner and L. Eyring (North-Holland, Amsterdam, 1979), Vol. 2, Chap. 19.
- <sup>5</sup>T. Kasuya and D. X. Li, *J. Magn. Magn. Mater.* **167**, L1, (1997); *Physica B* **230–232**, 472 (1997).
- <sup>6</sup>A. G. Petukhov, W. R. L. Lambrecht, and B. Segall, *Phys. Rev. B* **53**, 4324 (1996).
- <sup>7</sup>A. Hasegawa and A. Yanase, *J. Phys. Soc. Jpn.* **42**, 492 (1977).
- <sup>8</sup>C. M. Aerts, P. Strange, M. Horne, W. H. Temmerman, Z. Szotek, and A. Svane, *Phys. Rev. B* **69**, 045115 (2004).
- <sup>9</sup>W. R. L. Lambrecht, *Phys. Rev. B* **62**, 13538 (2000).
- <sup>10</sup>G. Busch, *J. Appl. Phys.* **38**, 1386 (1967).
- <sup>11</sup>T. R. McGuire, R. J. Gambino, S. J. Pickart, and H. A. Alperin, *J. Appl. Phys.* **40**, 1009 (1969).
- <sup>12</sup>R. J. Gambino, T. R. McGuire, H. A. Alperin, and S. J. Pickart, *J. Appl. Phys.* **41**, 933 (1970).
- <sup>13</sup>W. Stutius, *Phys. Kondens. Mater.* **10**, 152 (1969).
- <sup>14</sup>R. A. Cutler and A. W. Lawson, *J. Appl. Phys.* **46**, 2739 (1975).
- <sup>15</sup>D. X. Li, Y. Haga, H. Shida, T. Suzuki, T. Koide, and G. Kido, *Phys. Rev. B* **53**, 8473 (1996).
- <sup>16</sup>D. X. Li, Y. Haga, H. Shida, T. Suzuki, and Y. S. Kwon, *Phys. Rev. B* **54**, 10483 (1996).
- <sup>17</sup>H. Yamada, T. Fukawa, T. Muro, Y. Tanaka, S. Imada, S. Suga, and T. Suzuki, *J. Phys. Soc. Jpn.* **65**, 1000 (1996).
- <sup>18</sup>F. Hulliger, in *Handbook of Physics and Chemistry of Rare Earths*, edited by K. A. Gschneidner and L. Eyring (North-Holland, Amsterdam, 1979), Vol. 4, Chap. 33.
- <sup>19</sup>T. Kasuya, *IBM J. Res. Dev.* **14**, 214 (1970); *CRC Crit. Rev. Solid State Sci.* **3**, 131 (1972).
- <sup>20</sup>S. Methfessel and D. C. Mattis, *Magnetic Semiconductors* (Springer, Berlin, 1968).
- <sup>21</sup>G. A. Sawatzky, W. Geertsma, and C. Haas, *J. Magn. Magn. Mater.* **3**, 37 (1976).
- <sup>22</sup>B. T. Thole, P. Carra, F. Sette, and G. van der Laan, *Phys. Rev. Lett.* **68**, 1943 (1992); P. Carra, B. T. Thole, M. Altarelli, and X. Wang, *ibid.* **70**, 694 (1993).
- <sup>23</sup>E. Goering, A. Fuss, W. Weber, J. Will, and G. Schütz, *J. Appl. Phys.* **88**, 5920 (2000).
- <sup>24</sup>R. Nakajima, J. Stöhr, and Y. U. Idzerda, *Phys. Rev. B* **59**, 6421 (1999).
- <sup>25</sup>F. Leuenberger, A. Parge, and W. Felsch (unpublished).
- <sup>26</sup>L. W. Roeland, G. J. Cock, F. A. Muller, C. A. Moleman, K. A. M. McEwen, R. C. Jordan, and D. W. Jones, *J. Phys. F: Met. Phys.* **5**, L233 (1975).
- <sup>27</sup>A. Arrott, *Phys. Rev.* **108**, 1394 (1957); A. Arrott and J. E. Noakes, *Phys. Rev. Lett.* **19**, 786 (1976).
- <sup>28</sup>R. Schiller and W. Nolting, *Solid State Commun.* **110**, 121 (1999); R. Schiller, W. Müller, and W. Nolting, *Phys. Rev. B* **64**, 134409 (2001).
- <sup>29</sup>M. R. Oliver, J. O. Dimmock, and T. B. Reed, *IBM J. Res. Dev.* **14**, 276 (1970); S. von Molnar, *ibid.* **14**, 269 (1970); M. R. Oliver, J. A. Kafalas, J. O. Dimmock, and T. B. Reed, *Phys. Rev. Lett.* **24**, 1064 (1970).
- <sup>30</sup>Y. Shapira, S. Foner, and T. B. Reed, *Phys. Rev. B* **8**, 2299 (1973); Y. Shapira, S. Foner, R. L. Aggarwal, and T. B. Reed, *ibid.* **8**, 2316 (1973).
- <sup>31</sup>M. R. Oliver, J. O. Dimmock, A. L. McWhorter, and T. B. Reed, *Phys. Rev. B* **5**, 1078 (1972).
- <sup>32</sup>J. B. Torrance, M. W. Shafer, and T. R. McGuire, *Phys. Rev. Lett.* **29**, 1168 (1972).
- <sup>33</sup>The spectrum shown here for an uncovered GdN layer remains unaltered after deposition of a 30 Å thick Cr cap layer and after subsequent partial removal of it by Ar ion etching, a procedure employed for the XA and XMCD measurements (see Sec. II).
- <sup>34</sup>The calculated GdN density of states (unpublished results, not contained in Ref. 8) was provided by C. M. Aerts *et al.*
- <sup>35</sup>A relaxation energy of about 6 eV has been calculated for praseodymium by W. M. Temmerman, Z. Szotek, and H. Winter, *Phys. Rev. B* **47**, 1184 (1993). However, to assume that a similar value might be effective in GdN is not justified since a variation across the rare-earth series cannot be excluded.
- <sup>36</sup>D. E. Eastman, F. Holzberg, and S. Mathfessel, *Phys. Rev. Lett.* **23**, 226 (1969).
- <sup>37</sup>B. T. Thole, G. van der Laan, J. C. Fuggle, G. A. Sawatzky, R. C. Karnatak, and J.-M. Esteve, *Phys. Rev. B* **32**, 5107 (1985); J. B. Goedkoop, B. T. Thole, G. van der Laan, G. A. Sawatzky, F. M. F. de Groot, and J. C. Fuggle, *ibid.* **37**, 2086 (1988).
- <sup>38</sup>J. Holroyd, Y. Idzerda, and S. Stadler, *J. Appl. Phys.* **95**, 6571 (2004).
- <sup>39</sup>A. Rogalev, J. Goulon, and C. Brouder, *J. Phys.: Condens. Matter* **11**, 1115 (1999).
- <sup>40</sup>P. G. Steeneken, Ph.D. thesis, chap. 6, University of Groningen, 2002; <http://www.ub.rug.nl/eldoc/dis/science/p.g.steeneken/>
- <sup>41</sup>G. Schütz, W. Wagner, W. Wilhelm, P. Kienle, R. Zeller, R. Frahm, and G. Materlik, *Phys. Rev. Lett.* **58**, 737 (1987).
- <sup>42</sup>J. I. Igarashi and K. Hirai, *Phys. Rev. B* **50**, 17820 (1994).
- <sup>43</sup>H. Ebert, *Rep. Prog. Phys.* **59**, 1665 (1996).
- <sup>44</sup>G. Y. Guo, *J. Phys.: Condens. Matter* **8**, L747 (1996); *Phys. Rev. B* **55**, 11619 (1997).
- <sup>45</sup>M. Takahashi and J. I. Igarashi, *Phys. Rev. B* **67**, 245104 (2003).
- <sup>46</sup>F. Leuenberger *et al.*; the spectra are not presented here in view of their preliminary nature.
- <sup>47</sup>B. N. Harmon and A. J. Freeman, *Phys. Rev. B* **10**, 1979 (1974); J. C. Lang, X. Wang, V. P. Antropov, B. N. Harmon, A. I. Goldman, H. Wan, G. C. Hadjipanayis, and K. D. Finkelstein, *ibid.* **49**, 5993 (1994).
- <sup>48</sup>P. G. Steeneken, L. H. Tjeng, I. Elfimov, G. A. Sawatzky, G. Ghiringhelli, N. B. Brookes, and D.-J. Huang, *Phys. Rev. Lett.* **88**, 047201 (2002).